

In August 2015 we were awarded 15 shifts on ID27 to study melting phase relations of a range of compositions in the MgO-SiO₂ and CaO-MgO-SiO₂ systems at pressures relevant for Earth's lower mantle (24-134 GPa) using new metal-encapsulated setup for laser-heated diamond anvil cell (LH-DAC) experiments. However, due to quite refractory character of the compositions in the simple binary and ternary, hence relatively high melting temperatures required to study melting phase relations at extreme pressures, we have decided to focus on studying melting phase relations of natural basalt (Icelandic Basalt, BIR-1) instead. In this report we summarize the further development of the experimental method prior to the beamtime (§1) and some preliminary results of the diffraction patterns obtained during the beamtime (§2).

1. Methodological advancements of the experimental setup

At the stage of the application for the beamtime (September 2014) the metal-encapsulated samples were fabricated as described in proposal No. 36417. However, due to further technological development and additional tests carried at our home laboratory at the School of Earth Sciences in Bristol, the method of metal-encapsulation of the silicate samples improved and prior to the beamtime in August 2015 it involved few more preparations steps which are schematically illustrated in **Fig. 1** and in the text below.

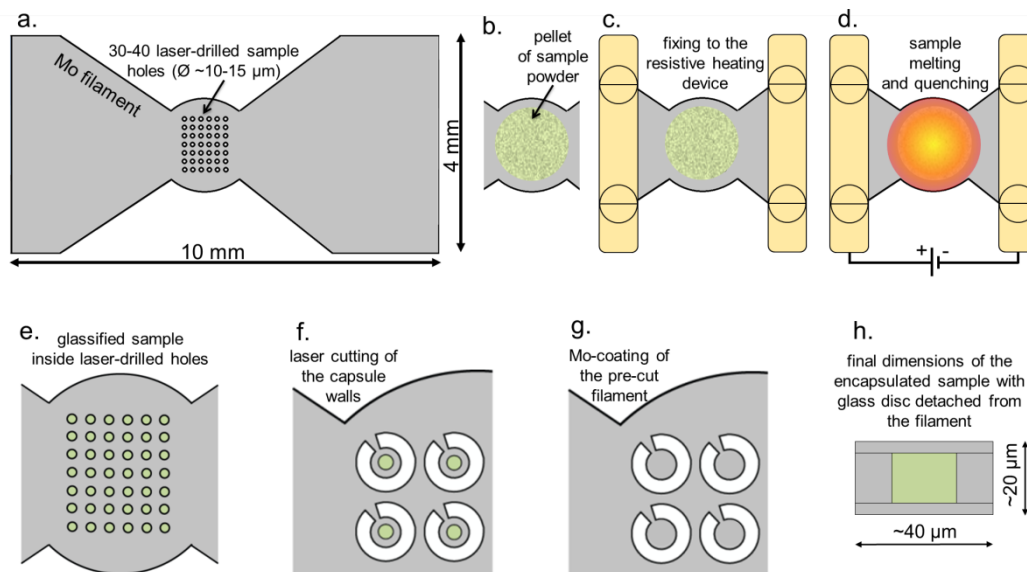


Figure 1. A schematic detailing the fabrication technique for the metal encapsulated glass disc samples using the so called ‘filament method’. See main text for more detail explanation.

In brief, the capsule preparation starts with manufacturing a metal filament made of 10 µm thick pure metal foil (e.g. Mo) of bow-tie shape (**Fig. 1a**) with a grid of 40-70 sample chambers of 10-15 µm diameter which are laser-drilled in the middle of the filament. Subsequently, a pressed pellet of powdered starting material is fixed on the neck of the Mo-filament on top of the drilled sample chambers (**Fig. 1b**). The assemblage is then connected with the resistive heating device (**Fig. 1c**) under Ar gas flow. The electrical power is increased manually until the neck of the filament with sample pellet, starts to glow and the starting

material on top melts (**Fig. 1d**). The melt permeates into the holes of the Mo-filament and then is rapidly quenched to form a glass by switching off the power (**Fig. 1e**). Subsequently, the filament is detached from the electrodes and the residual glass on the top of the filament is stripped away. The glass-filled sample chambers are then cut almost free from the filament, leaving a thin (about 10-15 μm) wall of Mo around each sample and a small neck to ensure the pre-cut capsules remain attached to the filament (**Fig. 1f**). To finish the encapsulation, the filament is then coated on both sides by a 3-4 μm layer of pure Mo metal by magnetron sputtering deposition (**Fig. 1g**, Q150R S Rotary-Pumped Sputter Coater, Quorum Technologies). After detachment from the Mo-gasket by a manipulating needle, the encapsulated samples are ready to be loaded into the standard DAC assemblage. The final encapsulated glass disc samples are approximately 15-20 μm thick and 30-50 μm in diameter before pressurization (**Fig. 1h**)

All the laser heated diamond anvil cell (LH-DAC) experiments were performed in Princeton-type symmetric DACs with 250, 200 and 150 μm culet sizes. The setup of a typical DAC assemblage is illustrated in **Fig. 2**. In this study we have mainly used KCl as the pressure medium material. Gaskets made from 250 μm thick Re-foil, indented to about 30-40 μm thickness at 20-25 GPa were used to achieve relatively deep sample chambers, which were laser-drilled in the middle of the indentation. In order to accommodate the capsules and as much pressure medium as possible, the sample chambers were about 90 and 50 μm in diameter for 250 and 150 μm culets, respectively. Before sample loading, an approximately 10 μm thick disc of KCl was emplaced in the sample chamber, then an encapsulated sample detached from the Mo-filament was loaded onto the lower KCl disc. In order to keep the capsule in the centre of the assemblage and for pressure monitoring a few ruby spheres were added aside the encapsulated sample (**Fig. 2**). A second disc of KCl was loaded on top of the encapsulated sample and gently compacted by squeezing in between the anvils to ensure that the pressure medium fills the space and separates the sample circumference from the inner Re gasket wall.

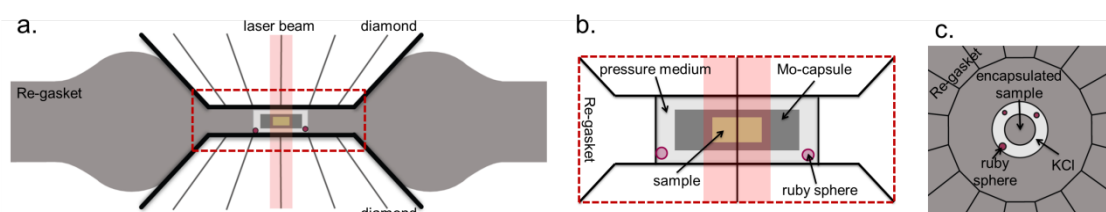


Figure 2. (a) A schematic cross section showing the experimental setup with an encapsulated sample loaded together with a few ruby spheres for pressure estimation and surrounded by KCl pressure medium inside the pre-indented Re-gasket. (b) Magnified view of the experimental configuration of the loaded encapsulated sample and laser heating area (red shaded) (c) Axial view of an encapsulated sample.

Before closing the cell and pressurization, each loaded DAC was heated at about 125 $^{\circ}\text{C}$ in the oven for at least an hour to remove adsorbed moisture. Final closing and initial compression were performed while the cell was still hot. Target pressure compression was aided by ruby fluorescence measurements.

Laser heating was performed from two sides with off-axis geometry and the heated spot was about 20-30 μm in diameter. The incandescent light from a $2 \times 2 \mu\text{m}^2$ area in the center of the laser-heated spot was selected using a pinhole and analysed spectroradiometrically to determine the temperature. In order to equalise the temperatures by varying the laser power on each side, we first tested the laser power versus temperature response in the 1500-2000 K range. This was required because only upstream side T-measurements were possible during XRD-collection. The downstream light-collecting optics for T-measurements had to be removed from the path of the diffracted X-ray detector (Schults et al., 2005). For more details of the beam-line setup see Mezouar et al. (2005).

A monochromatic incident X-Ray beam ($\lambda=0.3738 \text{ \AA}$) of about 3 μm size was co-aligned with the center of the laser-heated area by X-ray induced fluorescence of the KCl pressure medium. Diffracted X-Rays were collected on a MAR345 image plate (MarResearch) with exposure times of 5–30 seconds. The distance between the sample and detector was calibrated with a LaB_6 standard (399.954 mm).

We aimed to laser-heat the samples with $\sim 150 \text{ K}$ steps and with collection of XRD patterns at each step, until loss of the diffraction signal caused by large-degree melting. Pressure at ambient and high temperature was determined from the thermal equations of state of the Mo capsule (Huang et al., 2016) using the method of

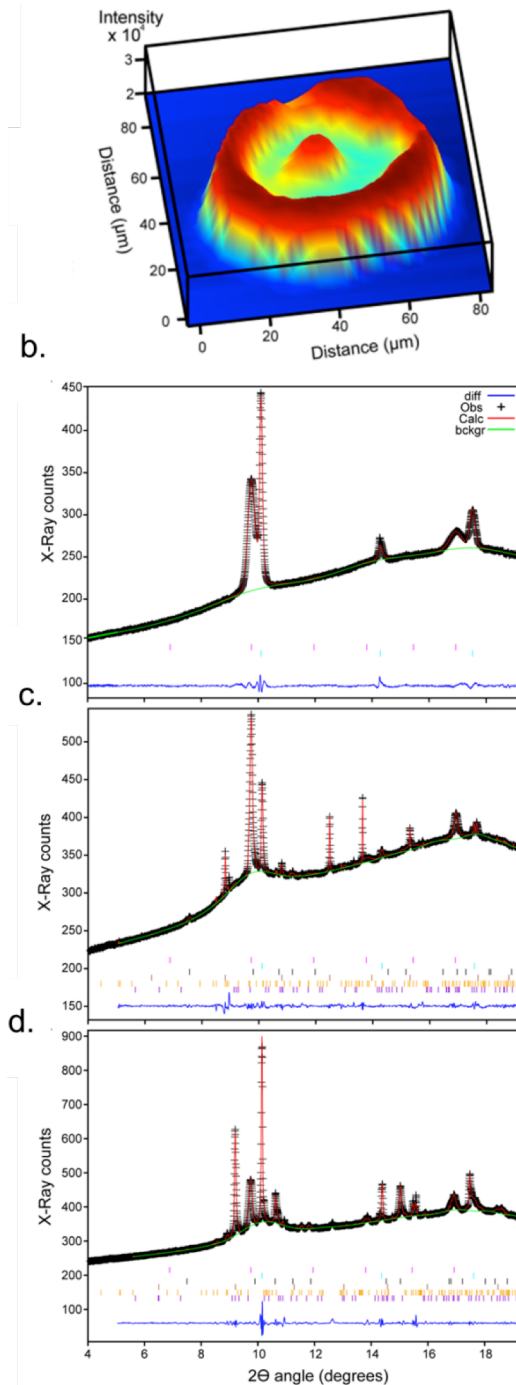


Figure 3. (a) A map of the Mo-encapsulated sample (elevated transmission in the middle) surrounded by Mo-walls of the capsule (low transmission region around the sample) surrounded by KCl pressure medium (elevated ring around the capsule). (b-d). Le Bail fits (red lines), backgrounds (green lines) and residuals (blue lines) for XRD data (black pluses) from a Mo-encapsulated BIR-1_3 sample before laser heating (b), in situ at 3130 K and (c) after quenching (d). The post heating pressure was 58 GPa. The tick marks represent reflections of, from top to bottom, KCl, Mo, stishovite, Ca-perovskite, calcium-ferrite structured phase, and bridgmanite.

Campbell et al. (2009). The 2-D diffraction patterns were subsequently integrated into 1-D diffraction patterns using the Fit2D (Hammersley, 1997) and Dioptas (Prescher and Prakapenka, 2015). The final diffraction patterns were fitted and interpreted using the Le Bail method (Le Bail et al., 1988) in the GSAS software package (Larson and Von Dreele, 1994 and Toby, 2001).

2. Preliminary results

In situ high-pressure and high-temperature experiments were performed with encapsulated glass disc samples of BIR-1 starting composition at pressures from 36 to 108 GPa and temperatures ranging from 2000 to almost 4000 K. At first, X-ray transmission maps of the pressurised samples were made in order to find the centre of the DAC assembly and precisely locate the glassy sample embedded in the Mo-capsule (**Fig. 3a**). Before laser heating a typical XRD pattern collected from encapsulated BIR-1 samples contained only peaks from Mo (capsule material) and KCl (pressure medium) (see **Fig. 3b**), confirming full vitrification of the starting material during sample preparation. With increasing laser power, the XRD patterns changed due to crystallization of characteristic phases including stishovite, Ca-perovskite, the calcium-ferrite structured Al-rich phase, and bridgmanite (**Fig. 3c,d**). After reaching sufficiently high temperatures we expected to see the disappearance of some of the phases accompanied by the diffuse scattering of the produced melt, but due to insufficient data and difficulties in reaching the extreme melting temperatures we were unable to perform more systematic study.

Moreover, due to technological limitations at the time of the sample preparation for the synchrotron experiments, the samples prepared for the *in situ* experiments were coated only with 1-2 μm layer of Mo which turned out to be insufficient for the mechanical stability of the capsule at extreme conditions, resulting in an unsustainable thermal environment. The encapsulated samples were also slightly bigger than described in §1.

Although the synchrotron-based study does not provide comprehensive documentation of the experimental products, it is worth mentioning that the quality of the obtained XRD spectra is very high and that the crystallizing phases are readily resolved, even though the sample quantity is much smaller than the pressure medium (KCl) and Mo-coating. This provides good evidence that metal-encapsulated samples can be successfully studied by *in situ* synchrotron-based XRD and more systematic study of the melting phase relations of the simpler and more complex composition is planned in the future.

After laser-heating and decompression, some of the successfully laser-heated samples were recovered and excavated by focused ion beam (FIB) milling and subsequently analysed by transmitted electron microscopy (TEM).

In the TEM sections of basaltic samples we found grains of bridgmanite, Ca-perovskite, stishovite and an Al-rich phase (probably: NAL-phase). Additional small Fe metal droplets were found and could have been a result of iron redox disproportionation related to the incorporation of the $\text{Fe}^{3+}\text{AlO}_3$ component in bridgmanite (e.g. Frost et al., 2004 and Sinmyo et al, 2011). Because the crystals were too small for high-quality diffraction analyses of single

grains, the phase identification was only based on EDX chemical maps. Previously presented XRD (**Fig. 3 b-d**) data from the in situ experiments seems to confirm the observed phases.

The technological development and preliminary results presented in this report have been a part of the Marzena Anna Baron's PhD thesis entitled 'Experimental constraints on Earth's lower mantle melting and core formation' at the University of Oslo and University of Bristol and are also planned for further publication (Baron et al, (in prep.)).

References:

Baron, M.A., Lord, O.T., Thielmann, M., Drewitt, J.W.E., Wang, W., Petitgirard, S., Miyajima, N., Frost, D.J., Badro, J., Garbarino, G., Trønnes, R.G., Walter, M.J. (in prep.) Metal-encapsulation of silicate samples for LH-DAC experiments at lower mantle conditions – technical development, preliminary results and numerical modelling of the thermal distribution.

Campbell, A.J., 2008. Measurement of temperature distributions across laser heated samples by multispectral imaging radiometry. *Rev. Sci. Instrum.* 79, 015108.

Frost, D.J., Liebske, C., Langenhorst, F., McCammon, C.A., Trønnes, R.G., Rubie, D.C., 2004. Experimental evidence for the existence of iron-rich metal in the Earth's lower mantle. *Nature* 428, 409-412.

Hammersley, A.P., 1997. FIT2D: an introduction and overview. ESRF Technical Report ESRF-97-HA-02T, Grenoble, France.

Huang, X., Li, F., Zhou, Q., Meng, Y., Litasov, K.D. Wang, X., Liu, B., Cui, T., 2016. Thermal equation of state of Molybdenum determined from in situ synchrotron X-ray diffraction with laser-heated diamond anvil cells. *Scientific Reports* 6, Article number: 19923.

Larson, A.C., Von Dreele, R.B., 1994. General Structure Analysis System (GSAS). Los Alamos National Laboratory Report LAUR 86-748

Le Bail, A., Duroy, H., Fourquet, J.L., 1988. Ab-initio structure determination of LiSbWO₆ by X-ray powder diffraction. *Mater. Res. Bull.* 23, 447-452.

Mezouar, M., Crichton, W.A., Bauchau, S., Thurel, F., Witsch, H., Torrecillas, F., Blattman, G., Marion, P., Dabin, Y., Chevanne, J., Hignette, O., Morawe, C., Borel, C., 2005. Development of a new state-of-the-art beamline optimized for monochromatic single-crystal and powder X-ray diffraction under extreme conditions at the ESRF. *J. Synchrotron Radiation* 12, 659-664.

Prescher, C., Prakapenka, V.B., 2015. DIOPTAS: a program for reduction of two-dimensional X-ray diffraction data and data exploration. *High Press. Res.* 35:3, 223-230. Prescher and Prakapenka, 2015

Schultz, E., Mezouar, M., Crichton, W., Bauchau, S., Blattmann, G., Andraut, D., Fiquet, G., Boehler, R., Rambert, N., Sitaud, B., Loubeyre, P., 2005. Double-sided laser heating system for in situ high pressure-high temperature monochromatic X-ray diffraction at the ESRF. *High Press. Res.* 25:1, 71-83.

Sinmyo, R., Hirose, K., Muto, S., Ohishi, Y., Yasuhara, A., 2011. The valence state and partitioning of iron in the Earth's lowermost mantle. *J. Geophys. Res.* 116, B07205.

Toby, B.H., 2001. EXPGUI, a graphical user interface for GSAS. *J. Appl. Crystallogr.* 34, 210-213.